Article

Whiting (*Merlangius merlangus*) Grows Slower and Smaller in the Adriatic Sea: New Insights from a Comparison of Two Populations with a Time Interval of 30 Years

Federico Calì [1,2,3,4,*], Federica Stranci [3], Mario La Mesa [4], Carlotta Mazzoldi [3], Enrico Arneri [2] and Alberto Santojanni [2]

1   Department of Biological, Geological, and Environmental Sciences (BiGeA), Alma Mater Studiorum—University of Bologna, 40126 Bologna, Italy
2   National Research Council—Institute for Marine Biological Resources and Biotechnologies (CNR-IRBIM), 60125 Ancona, Italy; enrico.arneri@cnr.it (E.A.); alberto.santojanni@cnr.it (A.S.)
3   Department of Biology, University of Padova, 35121 Padova, Italy; fstranci@gmail.com (F.S.); carlotta.mazzoldi@unipd.it (C.M.)
4   National Research Council—Institute of Polar Sciences (CNR-ISP), 40129 Bologna, Italy; mario.lamesa@cnr.it
*   Correspondence: federico.cali2@studio.unibo.it

Abstract: Nowadays, overexploitation and climate change are among the major threats to fish production all over the world. In this study, we focused our attention on the Adriatic Sea (AS), a shallow semi-enclosed sub-basin showing the highest exploitation level and warming trend over the last decades within the Mediterranean Sea. We investigated the life history traits and population dynamics of the cold-water species whiting (*Merlangius merlangus*, Gadidae) 30 years apart, which is one of the main commercial species in the Northern AS. The AS represents its southern limit of distribution, in accordance with the thermal preference of this cold-water species. Fish samples were collected monthly using a commercial bottom trawl within the periods 1990–1991 and 2020–2021. The historical comparison highlighted a recent reduction in large specimens (>25 cm total length, TL), which was not associated with trunked age structures, therefore indicating a decrease in growth performance over a period of 30 years ($L_{\infty 90-91} = 29.5$ cm TL; $L_{\infty 20-21} = 22.8$ cm TL). The current size at first sexual maturity was achieved within the first year of life, at around 16 cm TL for males and 17 cm TL for females. In the AS, whiting spawns in batches from December to March, showing a reproductive investment (gonadosomatic index) one order of magnitude higher in females than in males. Potential fecundity (F) ranged from 46,144 to 424,298, with it being heavily dependent on fish size. We hypothesize that the decreased growth performance might be related to a metabolic constraint, possibly related to the increased temperature and its consequences. Moreover, considering the detrimental effects of size reduction on reproductive potential, these findings suggest a potential endangerment situation for the long-term maintenance of whiting and cold-related species in the AS, which should be accounted for in setting management strategies.

Keywords: Adriatic Sea; whiting; otolith; growth models; cold-water species; demersal resources; bottom trawling

Key Contribution: The comparison of growth performance between the 1990–1991 and 2020–2021 populations of whiting collected in the Northern Adriatic Sea revealed a decline in the maximum size not coupled with decreased age, supporting the hypothesis of metabolic constraints due to sea warming, which is particularly high in the study area. The Adriatic population of whiting shows a faster growth rate and shorter life cycle compared to the other basins of the Mediterranean Sea and the Atlantic Ocean.

1. Introduction

During the last century, marine fish species have suffered increasing levels of impact due to human activity, such as habitat degradation and fishing exploitation. Meanwhile, climate change has produced great modifications in marine ecosystems, e.g., changing species distributions and trophic dynamics [1–4]. The dramatic and long-term effects of overfishing have been widely reported all over the world, leading to altered and less productive ecosystems [5–8]. Overfishing is considered the primary cause of the decline in marine populations, and its consequences on ecosystems started occurring centuries ago. In particular, analyses of historical data have revealed that a stronger decline has been observed for large-sized, long-lived, and late sexual maturing species, such as large marine vertebrates [9]. Among bony fish, the Atlantic cod, *Gadus morhua* Linnaeus, 1758, underwent the most dramatic collapse in the early 1990s in the north western Atlantic Ocean, also determining strong negative impacts on socio-economic systems [10]. On the other hand, over the 21st century, increasing evidence of the significant role of sea warming in affecting fish ecology and fishing yields has been provided. In response to increased temperatures, marine organisms have shifted their distribution ranges (generally towards higher or colder latitudes), changed their phenology, and reduced their body size [11,12]. Despite this, the net effect of these changes on species abundance is not only determined by the specific thermal tolerance but is also dependent on the ecoregion, taxonomy, and exploitation history [13–15]. Accordingly, temperate fish (experiencing strong seasonal variation) are expected to be more tolerant compared to their polar and tropical counterparts, which are adapted to stable cold and warm environments, respectively [16]. Moreover, marine organisms are often subjected to both fishery exploitation and climate change, which may play synergistic or antagonistic roles depending on the context, and disentangling their effects is often difficult [17–20].

The Mediterranean Sea has been defined as a sea "under siege" [21], because of its long history of exploitation and the higher rate of water warming compared to other marine regions [3,22]. It is considered a biodiversity hotspot, hosting more than 17,000 species, many of them endemic to the Mediterranean area [21]. The contemporary presence of high species diversity and multiple sources of impact determines an increasing concern about the management of fish resources in relation to the current level of fishing exploitation. It was recently highlighted that 90% of the Mediterranean commercial stocks were assessed as being out of safe biological limits [22]. In addition, rapid sea warming, combined with the expansion of non-indigenous species, is modifying the habitat suitability for commercial species, with detrimental effects on their resilience to fishing [23–25]. Despite the introduction of regulations according to the European (EU) Common Fisheries Policy and Regulation 1967/2006 in EU countries (e.g., fishing capacity and effort limitations, regulation of mesh size, and spatial/temporal closures), Mediterranean resources have not shown signs of recovery [22]. The failure of fisheries policies is mainly related to a low level of compliance and non-enforcement of rules in the whole Mediterranean area, where there has always been a disagreement between scientific advice and national management plans [26]. Moreover, increasing evidence is showing that climate change affects the productivity potential of fish stocks at a global scale [14], suggesting a significant role of environmental factors in the failure to recover fish resources. The colder regions (high latitude) show higher vulnerability and economic loss from climate change, particularly in shallow and enclosed basins, which could be less resilient to climate and human stressors [15].

The Adriatic Sea (AS) is the basin showing the highest exploitation and sea warming rate in the Mediterranean Sea, making it an ideal model to study the simultaneous effects of fishing and climate change on fish species [6,15,27]. This semi-enclosed basin represents the northernmost part of the Mediterranean Sea; it is subjected to the cold Bora wind (with the north east direction) and receives cold water from many alpine rivers, determining a suitable habitat for those species typical of the Atlantic waters, the so-called "boreal species" [28,29]. An example is represented by the whiting, *Merlangius merlangus* (Linnaeus, 1758) (Gadidae), a benthopelagic species widespread mainly in the northeastern Atlantic

Ocean and in the northern sub-basins of the Mediterranean and Black Seas (Adriatic, Aegean, Marmara, and Azov Sea). Despite its commercial importance at a local scale, with it being one of the main bony fish resources caught by bottom trawlers, the biological traits of this species in the AS are still poorly known [30,31], and most of the available literature comes from the Atlantic Ocean and the Black Sea. Knowledge of fish biology is essential to estimate the vulnerability and resilience to the external stressor of the fish species already assessed, as well as to increase the number of species to be assessed, which is currently less than 5% of the fish species worldwide [32]. This is particularly true for exploited species with narrow geographical ranges whose biological traits and population dynamics may differ between geographical areas depending on the environmental, ecological, and fishing features.

This work aims to investigate the life history traits of *M. merlangus* in the Northern AS (NAS), focusing on the historical comparison of two populations sampled in the same area with a time interval of 30 years. Population dynamics and age/length structures were examined through length–frequency distributions (LFDs) analysis and otolith readings, respectively. We investigated the reproductive cycle and fecundity to provide information useful to shed light on the life cycle of this species in the NAS. The historical comparison enabled us to infer about the effect of fishing or environmental changes on the growth performance and reproductive potential of this species. To evaluate the phenotypic plasticity and spatial variation of whiting life history traits, in the discussion, we compared our data with the Atlantic Ocean and Black Sea populations. Considering the potential vulnerability of whiting due to the combined effect of overexploitation and sea warming, the further aim of this study was to provide new insights to underpin more comprehensive management strategies under an ecosystem approach.

2. Materials and Methods

2.1. Study Area

The study area comprises the northern part of the AS, a semi-enclosed basin located in the Central Mediterranean Sea (Figure 1). Based on the bathymetric differences along its latitudinal axis, three sub-basins can be identified and are roughly characterized by sandy shores on the western side and rocky shores and islands on the eastern side [33]. The northern sub-basin encompasses the northernmost part down to the 100 m bathymetric line and is characterized by an extremely shallow mean depth (about 30 m) and strong river runoffs. Indeed, Po and the other northern Italian rivers are the source of about 20% of the total Mediterranean river runoff [34,35]. Primary productivity is very high along the northwestern side and decreases southward and eastward due to the scarcity of rivers along the Croatian coastline [36]. The sea bottom temperature shows a strong seasonal cycle in winter and summer, ranging from 7 to 27 °C and from 10 to 18 °C in coastal and deep waters, respectively [37]. The physical properties and dynamics of the area are strongly influenced by atmospheric forces and river discharge, displaying marked temporal and spatial variations [33,38].
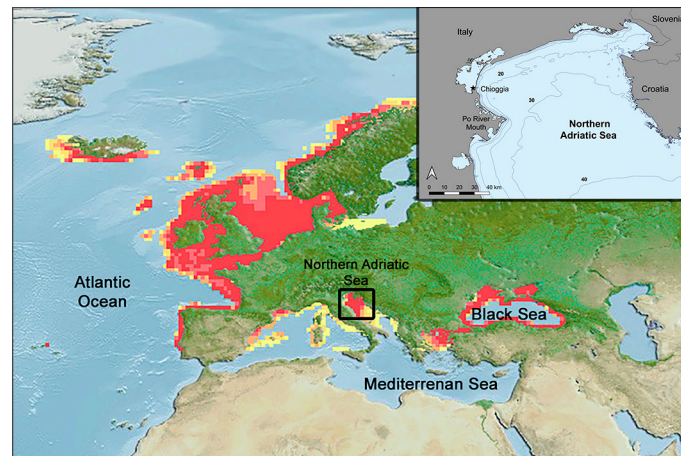
Figure 1. Distribution range of *Merlangius merlangus* and study area (black square). The color intensity from yellow to red indicates the probability of occurrence (modified from [39]). Top right square: detailed map of the study area with bathymetric lines, showing the location of Chioggia's port (★) and the Po River mouth.

2.2. Sampling Design and Population Parameters

The fish samples were collected monthly in the same fishing ground in front of the Po River mouth during two different sampling periods (1990–1991 and 2020–2021). The first was carried out between March 1990 and December 1991; the second one was carried out between November 2020 and November 2021. No samples were available from February and May 1990–1991 and from August of both periods due to the annual ban on trawling activities. The fish samples were caught using an Italian-type commercial fishing net (otter bottom trawl, *tartana*) with a cod-end mesh size of 40 mm, towed between 15 and 35 m depth. In 2020–2021, juveniles were collected bi-weekly from April to June, aiming to thoroughly assess the timing and duration of recruitment. Moreover, when sampling on board was not possible, whiting samples were collected at the landing sites of the Chioggia trawling fleet from local fishers exploiting the same fishing ground. All of the sampled individuals were measured to the nearest half cm (total length, TL) to obtain the length frequency distributions (LFD) of each sample. A monthly subsample of 40–60 specimens representative of the whole size range was randomly selected for biological examination. The following measures were taken: TL to the nearest mm, total weight (TW) to the nearest 0.1 g, and gonad weight (GW, only in the 2020–2021 sample) to the nearest 0.01 g. Sex was assigned macroscopically in specimens > 12 cm TL, and only in the 2020–2021 sample the gonad maturity stage was evaluated using the standard ICES (2008) six-point scale: (1) immature; (2) maturing; (3) spawning; (4) spent; (5) and resting/skip of spawning; (6) abnormal. Since it was not possible to determine the sex macroscopically in individuals smaller than 12 cm TL, they were treated as unsexed juveniles. The sagittal otoliths were removed, cleaned, and stored dry in vials for ageing purposes. Sex ratios, expressed as the percentage of females in relation to the number of males, were calculated and the difference between the sampling periods was tested using a χ^2 test for proportions. The condition factor (K) was calculated using the following relationship, K = 10^3 (TW/TL^b), where b is 3 or $\neq$3 in the case of isometric or allometric growth, respectively [40]. Differences in K values between the two samplings were tested by the Mann–Whitney test.

To assess the reproductive investment in gonads, the GW was used to calculate the gonadosomatic index (GSI = GW/TW × 100). In 2020–2021, the ovary subsamples were weighed and fixed in 10% seawater formaldehyde for fecundity estimation in pre-spawning females from the whole size range. Furthermore, ovaries from stage 2/3 females were stored in Dietrich solution (900 mL distilled water, 450 mL 95% ethanol, 150 mL 40% formaldehyde, and 30 mL acetic acid) for histological analyses.

2.3. Age Estimation

From the whole fish sample, a representative subsample was selected for each sampling period, grouping specimens in 1 cm TL classes. Age readings were performed on two males and two females per length class in each monthly sample to fully represent the population size range. The morphology of whiting sagittal otoliths makes age readings difficult on the whole otolith because of the thickness and the presence of bumps (Figure 2).
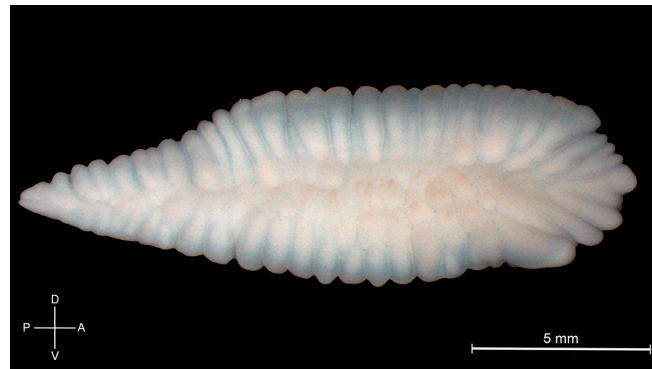
Figure 2. Right otolith of *Merlangius merlangus*, distal side view. D = dorsal axis; A = anterior axis; V = ventral axis; P = posterior axis.

An opacification process was noticed during dry storage, in that the otoliths of the individuals sampled in 1990–1991 were homogeneously white. After several trials, the "burning and breaking" technique was considered the most appropriate to establish a reliable age estimate [41], removing the opacification effect and enhancing the annulation pattern in the otoliths from both sampling periods. The otoliths were burnt in an oven at 350 °C for 2–4 min (depending on size), embedded in resin (Crystalbond 509 Amber, Aremco products, Inc., New York, USA), ground using an abrasive paper, and polished on a lapping film with 0.05 μm alumina powder. Particular attention was given to obtaining a final reading plane passing across the nucleus, using the shape of *sulcus acusticus* as a reference. The otolith sections were fixed onto glass slides using resin and soaked in fresh water over a dark background to enhance the contrast between the translucent and opaque zones. The otolith readings were performed under reflected light, counting the rings from the nucleus to the distal margin of the section. The sections were read using a stereomicroscope (Leica MZ6) at low magnification (10×). Age was estimated as the number of completely formed annuli, consisting of one opaque and one neighboring translucent ring. The samples were blindly read twice and in random order by two operators independently, without any indication of the date of capture, sex, or fish size. The age and the edge type (translucent or opaque) of each otolith sample were recorded and, in case of disagreement between the readers, the sample was discarded. The edge condition (percentage of otoliths with an opaque margin each month) was analyzed to determine the periodicity and timing of ring formation, allowing the annual formation of the rings to be verified. To evaluate the ageing precision [42], the index of average percent error (APE) [43] and the mean coefficient of variation (CV) [44] were calculated by comparing readings within and between readers. Given the low number of classes, the age was estimated in months, establishing a conventional common birth date (1 January) according to the reproductive period [30] and considering the capture date and the edge type. Since we observed an opaque deposition in fish smaller than 12 cm only, they were considered young of the year (YOY), and their age was calculated taking into account only the month of capture.

The von Bertalanffy growth function (VBGF) was used to describe the growth of the population:

$$TL = L_\infty \left(1 - e^{-k(t-t_0)}\right)$$

where TL is the length-at-age t, L_∞ is the asymptotic total length, k is the so-called Brody growth rate coefficient which determines how fast the fish approaches L_∞, and t_0 is the theoretical age at which the average length is zero. The VBGF was fitted to the observed length-at-age data pairs. The VBGF parameters were estimated for males, females, and sex combined, using Growth II software (PISCES Conservation Ltd., Lymington, UK). The unsexed juveniles were included in both female and male growth curves to improve the fitting of the model in the first period of growth. Differences in growth between the sampling periods and sexes were tested by applying the Kimura likelihood-ratio test [45]. The growth performance index ($\varphi = \log k + 2\log L_\infty$) was calculated to allow for comparison among the growth parameters estimated in different populations of whiting [46].

2.4. Fecundity and Maturity Estimation

Fecundity was estimated in spawning females (macroscopic stage 3; [47]) at the beginning of the spawning season (December 2020–2021), assuming that spawning had not yet occurred. The gravimetric method was used by counting the number of the most advanced oocytes in a weighted subsample [48], representing 1–2% of the GW. To assess any possible difference in oocyte density across the ovaries, three subsamples were taken from different portions of the ovary (anterior, median, and posterior) from five specimens, and oocyte counts were compared among the three portions. As no significant difference in the number of oocytes/g of the ovaries among the portions was found ($\chi^2 = 2.8$, *df* = 2, *p* = 0.24, Friedman test for related samples), the portion of the ovary used in fecundity estimation was randomly chosen. After at least 20 days of fixation, each ovary subsample was first treated with a mixture of commercial sodium hypochlorite (30%) and seawater (70%) [49] for 3 min to facilitate the disintegration of ovarian lamellae, and then, they were immersed in filtered sea water in a Petri dish with a dark background. The oocytes were manually spaced and photographed with a digital camera (Leica DFC 420) connected to a stereomicroscope at low magnification (8×), keeping the camera settings standard for all images. Then, ImagePro Plus version 6.0 imaging software (Media Cybernetics, Rockville, MD) was used to count and measure the oocytes semi-automatically, allowing the operator to check, modify, and set the measurement thresholds.

Pre-vitellogenic oocytes were identified and excluded from the counts, setting a threshold size of 150 μm, based on the histological analyses of ovaries. Following a standard protocol, the ovaries were taken from Dietrich solution, dehydrated, and embedded in paraffin wax (Paraplast®, Sigma-Aldrich, Burlington, NJ, USA). From each sample, transverse serial thin sections (7 μm) were mounted on slides and stained with Harris hematoxylin and eosin [50]. The tissue sections were observed under a light microscope (Leica DM4000B) using different magnifications to study oocyte development. Due to oocyte shrinkage during histological processing, a correction factor was applied to compare the diameters measured in the histological section with the formaldehyde-fixed ones [51].

With this species being a batch spawner with a "determinate" fecundity type [52], it was possible to estimate the potential fecundity (F), the relative potential fecundity (F_{rel}). and the batch fecundity (F_b). The potential fecundity (F), defined as the standing stock of vitellogenic oocytes [53], was estimated by applying the following equation:

$$F = (n/sw)\ GW,$$

where *n* is the number of vitellogenic oocytes in the subsample, *sw* is the weight of the subsample, and GW is the gonad weight. The F_b was calculated as the number of hydrated oocytes in the subsample multiplied by the ovary total weight. The F_{rel} and F_{brel} were then calculated as the number of vitellogenic and hydrated oocytes per gram of gutted body weight, respectively. The relationship between fish size and fecundity was assessed by applying a least squares regression analysis to $\log_{10}$-transformed data, applying the Shapiro–Wilk test to verify the assumptions of normality.

The size-at-first maturity TL_{50}, i.e., the size at which 50% of individuals are sexually mature, was estimated by taking into account 242 females and 196 males, collected between

November (when individuals in early maturation gonadal stages were observed) and March (when a few spawning individuals were still detected among post-spawner ones). Data on size and maturity stage were coupled to fit a predicted proportion of mature individuals (namely at stages 3 and 4) at size using a logistic model.

3. Results

3.1. Population Structure

From the collected samples, the total number of analyzed specimens for the age readings was 511 (180 males, 190 females, and 141 unsexed) out of 1895 specimens for 1990–1991 and 476 (209 males, 240 females, and 27 unsexed) out of 742 for 2020–2021. The sex ratio did not differ significantly between the samplings (two-sample Z-test for proportions, $\chi^2 = 1.54$, $df = 1$, $p = 0.21$), with the ratios being 0.52 and 0.55 for 1990–1991 and 2020–2021, respectively. In both samplings, females were dominant in the population.

The LFDs of the sexed subsamples are reported in Figure 3. The LFDs were rather different in the two sampling periods (two-sample Kolmogorov–Smirnov test, $p < 0.05$), clearly showing a higher number of individuals larger than 25 cm TL in 1990–1991 (Figure 3, left). The maximum size was higher in individuals caught in 1990–1991 (males: 30 cm TL, females: 37 cm TL) compared to 2020–2021 (males: 24 cm TL, females: 31 cm TL) (Figure 3; Mann-Whitney test, $p < 0.05$). In the 1990–1991 sample, the distribution was unimodal around 18 cm for both sexes and skewed toward larger sizes, whereas in 2020–2021, the modal class was 16 cm for males and 22 cm for females, showing divergent LFDs between the sexes. YOYs join the sampled population in April (at approximately 8 cm TL), producing a bimodal distribution in the LFD and showing fast growth over the spring and summer, with a mean growth of 3 cm TL per month (Figure A1).

(**a**) (**b**)
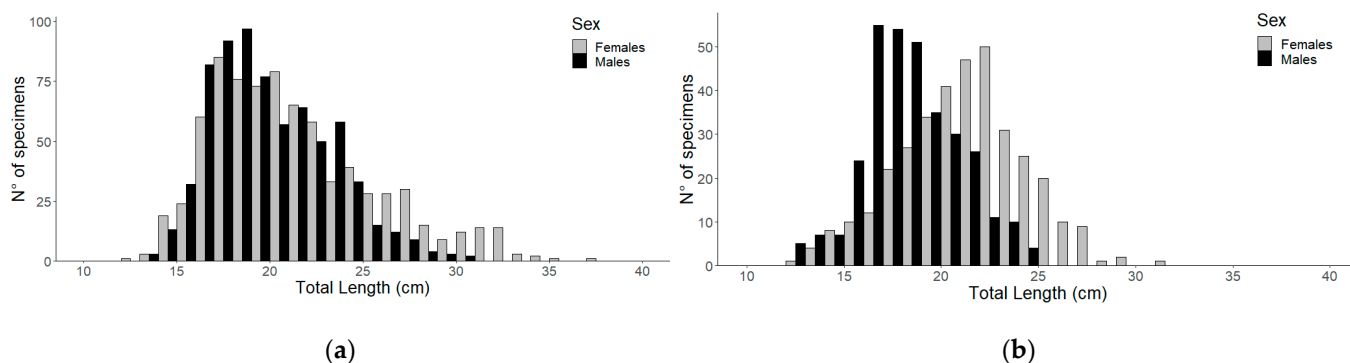
Figure 3. Length–frequency distribution (LFD) of the samples by sex. (**a**) 1990–1991 and (**b**) 2020–2021.

Comparing the mean condition factors (K) calculated for the same size classes (cm) in both sexes and sampling periods, they were higher in female individuals and in the 1990–1991 samples (Mann–Whitney test, $p < 0.05$).

3.2. Growth

The otolith edge-zone analysis throughout the year revealed that the opaque layer is laid during the warmer months, confirming the annual deposition of one opaque ring plus one translucent ring (Figures 4 and 5). A difference in the deposition timing of the opaque ring was detected between the sampling periods, ranging from April to September in the 1990–1991 samples and from May to July in the 2020–2021 ones.

The average percentage error (APE) and the coefficient of variation (CV) were low, at 0.9% and 1.3%, respectively, indicating high precision for the age readings. The age classes obtained from the otolith readings of the selected subsamples were three (age 0+, 1+, 2+); age estimates ranged from 2 to 32 months in the 1990–1991 samples and from 2 to 30 months in the 2020–2021 samples. The age–length keys of the two populations are reported in Tables 1 and 2. In Tables A1 and A2, the age-length keys for males, females,

and unsexed juveniles are reported. The year was divided into quarters to better visualize the population structure (quarters 3–9 = YOY; quarters 12–21 = 1+ age group; quarters 24–33 = 2+ age group). Significant differences were found in the mean sizes at age calculated for the two populations in both sexes (Wilcoxon signed-rank test; Z = 2.60, *p* < 0.01), with the 1990–1991 samples showing higher mean length-at-age than 2020–2021 across the whole age range.

Figure 4. Monthly edge composition indicating the proportion of the population with opaque margin otoliths (%, blue lines) and the number of individuals (bars) sampled. (**a**) 1990–1991 and (**b**) 2020–2021.

Figure 5. Transverse otolith section from a 2+ age class specimen (male, 28 cm TL) of *Merlangius merlangus* caught in October 1990, showing two completely formed annuli (black dots), consisting of one opaque and one neighboring translucent ring.

Table 1. Age–length for the combined sexes based on otolith readings of *Merlangius merlangus* sampled in the 1990–1991 period in the Northern Adriatic Sea. N = total number; SD = standard deviation; TL = total length.

Age (Quarters) Total Length (cm)	3	6	9	12	15	18	21	24	27	30	33	N
3	1											1
4	7											7
5	21											21
6	35											35
7	12											12
8	8											8
9	1	4										5
10	1	3										4

Table 1. *Cont.*

Age (Quarters) Total Length (cm)	3	6	9	12	15	18	21	24	27	30	33	N
11		6										6
12		8	1									9
13		22	4									26
14		41	14									55
15		6	8	2								16
16		5	8	2								15
17		7	8	4								19
18		7	8	5	2							22
19		8	8	6	3							25
20		5	8	8	4							25
21		4	8	9	6	1						28
22		3	7	7	5	1						23
23		1	7	8	6	2		1				25
24			4	3	5	4	1	3				20
25		1	1	4	3	2	3	2	1			17
26			4	8	5		2	3	1			23
27			1	4	5	4	2	2	1			19
28			1	2	2	3	2				1	11
29				1		3	1	1			1	7
30				1	1	3	1	1		1		8
31					1	2	1	1				5
32						2	2	3		1		8
33						1	1					2
34						1	1					2
35							1					1
37									1			1
N	86	131	100	74	48	29	18	17	4	2	2	511
TL mean (cm)	6.3	15.2	18.9	22.2	23.6	27.8	28.9	27.5	28.9	31.3	28.8	
TL SD	1.2	3.2	3.8	3.5	3.1	3.5	3.5	3.1	5.5	1.8	1.1	

Table 2. Age-length for the combined sexes based on otolith readings of *Merlangius merlangus* sampled in the 2020–2021 period in the Northern Adriatic Sea. N = total number; SD = standard deviation; TL = total length.

Age (Quarters) Total Length (cm)	3	6	9	12	15	18	21	24	27	30	33	N
3												0
4	1											1
5												0
6	13											13
7	15	1										16
8	11	2										13
9	5	2										7
10	2	2										4
11		3										3
12		6										6
13		10			1							11
14		9	2	4	3							18
15		5	7	10	10	2						34
16		7	6	10	12	2						37
17		8	8	12	11	3						42
18		4	7	11	15	6						43
19		1	5	12	10	7						35
20			8	9	10	10	1	3	1			42
21			3	8	10	9	2	3	2	1		38

Table 2. *Cont.*

Age (Quarters) Total Length (cm)	3	6	9	12	15	18	21	24	27	30	33	N
22			4	5	7	10	2	2	2	1		33
23			1	4	7	4	2	4	2			24
24				3	3	5		2	2			15
25				2	3	6	1	3	2			17
26					1	1		2	3	1		8
27						2		5	2			9
28						1		1				2
29								1				1
30						1		1		1		3
31								1				1
32												0
33												0
34												0
35												0
37												0
N	47	60	51	90	103	69	8	28	16	4	-	476
TL mean (cm)	7.7	14.4	18.5	19	19.2	21.6	22.6	25.5	24.2	27.9	-	
TL SD	1.2	2.8	2.4	2.8	2.9	3	1.6	3.6	2.2	5	-	

According to the likelihood ratio test on the estimated VBGF parameters, the 1990–1991 population showed higher values of L_∞ and lower values of k compared to 2020–2021 (Kimura likelihood ratio test, Tables 3 and 4). The growth performance index was higher in the 1990–1991 population, providing further evidence of a greater growth capability, as already highlighted by the mean length-at-age comparison. A higher overlap between the size ranges associated with each quarter was observed in 2020–2021 (Figure 6), in particular in the 1+ age group (quarters 12–24). As expected, considering the sexual dimorphism in size, males showed a lower L_∞ than females in both populations (Tables 3, A1 and A2).

Table 3. *Merlangius merlangus* von Bertalanffy growth parameters estimates for both sampling periods in the Northern Adriatic Sea. The growth rate coefficient (k) and theoretical age at which the average length is zero (t_0) are expressed in years^{-1} and years, respectively. L_∞ = asymptotic total length; φ = growth performance index.

	L_∞	k	t_0	φ
1990–1991 combined sexes	29.47	1.633	0.052	3.15
2020–2021 combined sexes	22.84	1.889	−0.043	2.99
1990–1991 females	35.14	1.219	0.045	3.17
2020–2021 females	25.11	1.663	−0.04	3.02
1990–1991 males	26.7	1.831	0.059	3.11
2020–2021 males	20.52	2.236	−0.02	2.97

Table 4. Kimura's likelihood ratio test results, used to compare the von Bertalanffy growth parameters estimates for both sexes and sampling periods of *Merlangius merlangus* from the Northern Adriatic Sea. L_∞ = asymptotic total length; k = growth rate coefficient.

		χ^2	*p*-Value
	L_∞	33.25	<0.01
1990–1991 vs. 2020–2021	k	1.1	0.29
	Whole model	255.78	<0.01
	L_∞	19.23	<0.01
Females vs. males 2020–2021	k	2.5	0.11
	Whole model	94.62	<0.01

Table 4. *Cont.*

		χ^2	*p*-Value
Females vs. males 1990–1991	L_∞	42.39	<0.01
	k	13.21	<0.01
	Whole model	80.07	<0.01
Females 2020–2021 vs. 1990–1991	L_∞	28.64	<0.01
	k	3.75	0.05
	Whole model	175.78	<0.01
Males 2020–2021 vs. 1990–1991	L_∞	29.16	<0.01
	k	1.45	0.23
	Whole model	177.69	<0.01

(**a**)   (**b**)
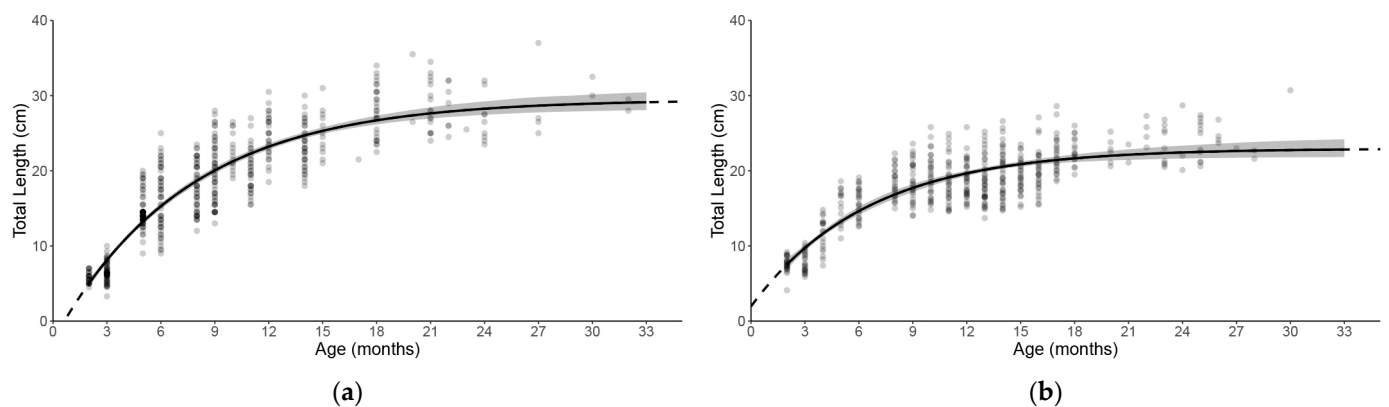
Figure 6. Von Bertalanffy growth models for the entirety of the 1990–1991 (**a**) and 2020–2021 (**b**) subsamples of *Merlangius merlangus* collected in the Northern Adriatic Sea.

3.3. Maturity Estimation and Fecundity

According to the macroscopic observation of gonad maturation and GSI monthly patterns, the spawning season extended from December to March, with stronger activity at the beginning of winter. During the spawning peak in December, the GSI mean value was 11% (max 18%) for females and 1% (max 3%) for males, showing a striking difference in the reproductive efforts between the sexes (Figure 7). Based on the logistic model fitted to the proportion of sexually mature specimens, size-at-first maturity L_{50} was estimated at 16.1 ± 0.1 cm TL for males and 16.8 ± 0.5 cm TL for females.

(**a**)   (**b**)
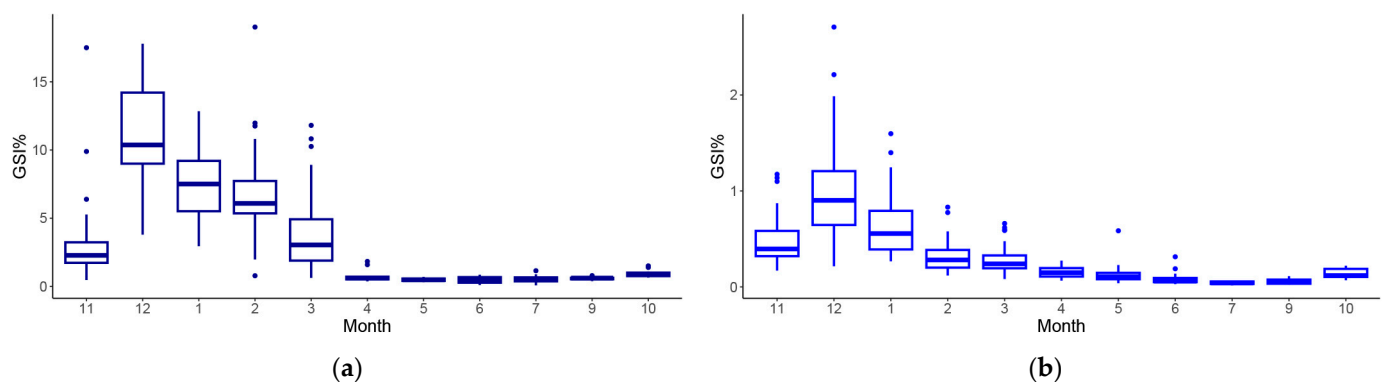
Figure 7. Monthly variation of the gonadosomatic index for *Merlangius merlangus* females (**a**) and males (**b**) across the 2020–2021 sampling.

A total of 15 females, ranging from 16.5 to 29 cm TL, were analyzed for fecundity estimation. Oocyte size frequency distributions (OFDs) in early spawning females indicated the presence of two or three modes corresponding to oocytes in different stages of

vitellogenesis. The first mode ranged in diameter from 100 to 450 μm, the second one ranged in diameter from 450 to 700 μm, and the third one was >700 μm, composed of hydrated oocytes. Different OFD patterns were observed in pre-spawning females depending on their gonadal development stage. Females in earlier developmental stages showed a higher overlap between the oocyte groups, while those in later stages showed a clear differentiation between modes (Figure 8). The maximum size of hydrated oocytes was 1300 μm in a 25 cm TL female.
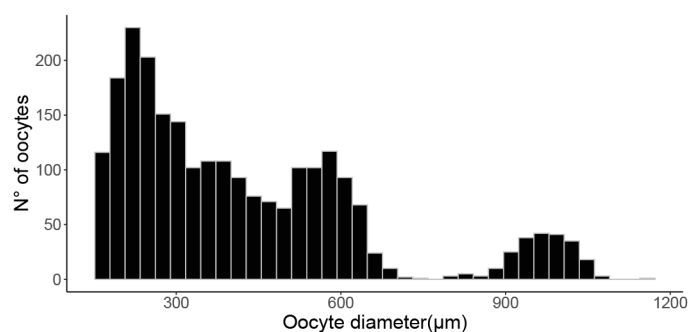
Figure 8. Size frequency distribution of vitellogenic oocytes for an early spawning female (macroscopic stage 3) showing three oocyte modes (TL = 20.6 cm).

The potential fecundity (F) ranged from 46,144 to 424,298 (201,035 ± 122,020) oocytes, and the relative potential fecundity (F_{rel}) ranged from 1362 to 3182 (2297 ± 546) oocytes g^{-1}. Batch fecundity was calculated on nine females, in which the mode of hydrated oocytes was markedly distinguishable from OFDs (Figure 8). Batch fecundity (F_b) ranged from 1293 to 22,949 (10,220 ± 6940), and the relative batch fecundity (F_{brel}) ranged from 31 to 206 (125 ± 63). The total number of vitellogenic oocytes was positively related to female size (TL) (F = 128, *df* = 14, *p* < 0.001). The relationship between TL and F is described by the equation:

$$F = 0.8795 \times TL^{3.95}; r^2 = 0.91$$

4. Discussion

The present study provides a comprehensive picture of the biological cycle of the *M. merlangus* stock in the NAS, focusing on the population structure, growth parameters, and reproductive traits. For this area, to our knowledge, the growth parameters and fecundity values have never been reported before. Moreover, this is the first time that populations sampled with a time-shift of 30 years from the same fishing ground are compared in terms of population structure and growth.

4.1. Historical Comparison

The temporal comparison revealed a reduction of the mean size over the considered period, with a higher proportion of large individuals in the 1990–1991 sample with respect to the 2020–2021 ones. This finding confirms the declining trend in size reported for several fish stocks at different latitudes mainly due to fishing exploitation [54]. Fishing affects ecosystems by removing selectively larger specimens of commercial species, determining short-term (e.g., removal of spawners from the stock) and long-term effects (e.g., selection of fast-growing and early maturing specimens) [18,55,56]. Nevertheless, since fishing exerts selective pressure by removing larger and, consequently, older individuals [57,58], it was expected for the same difference in the age structure to be observed. Conversely, our data revealed that in both populations, the maximum age was similar (30–32 months). An effect on mean size-at-age was observed instead, with higher sizes per age class in the 1990–1991 sample compared to the 2020–2021 ones. These results together suggest that the observed reduction in length classes is related to different growth performance, which may be explained by metabolic or trophic constraints.

The physiological performance of marine fish, with them being ectotherms, is tightly controlled by water temperature, and their essential body functions (growth and reproduction) are optimal only within the thermal tolerance of the species [59]. Oxygen consumption (i.e., metabolic rate) is higher in organisms living in warmer waters and it is proportional to body size [60]. Thus, as the water temperature increases, the maximum body size decreases to balance the increase in the metabolic rate [61,62]. Generally, the sensitivity to temperature changes in temperate species is low but it may vary depending on the specific location within its distribution range. Several studies have shown that under ocean warming, sensible species have been shifting their distribution towards higher latitudes and deeper waters to maintain physiological homeostasis [11,19]. However, sometimes a geographic constraint may prevent poleward migration, as in the case of enclosed seas, such as the Mediterranean Sea. Within this area, species distributions are highly clustered depending on the local features of water masses, and it is possible to find a wide range of species along the latitudinal axis: from the cold waters to the sub-tropical ones [63]. The coldest parts of the Mediterranean Sea are the Gulf of Lion and the NAS. Being located in the northern limit of the Mediterranean latitudinal range, these areas are defined as "cul-de-sacs", from which cold-water species will have no possibility of escaping. Recent observational data showed that the AS, and in particular the NAS, is the sub-basin with the highest warming trend in sea surface temperature in the Mediterranean Sea over the last 20 years [27,64] (Figure A2), which could determine a strong reduction in cold-adapted species during the ongoing century and, in the worst case scenario, even their local extinction [29]. This phenomenon is probably occurring in the Adriatic population of whiting, whose distribution is restricted to the central and northern parts of the sub-basin, showing high abundance only in the northern part [39]. Here, land boundaries could allow only a southward shift, which is prevented by the positive gradient of sea temperature and depth along the Adriatic latitudinal axis, creating a physical barrier. In fact, besides thermal tolerance, another peculiar feature of whiting is the preference for shallow waters, with the species being common at depths lower than 100 meters [65]. It is possible, therefore, to explain the observed difference in growth efficiency between populations in terms of a metabolic constraint due to the thermal tolerance of this species, limiting the increase in body size [59]. Moreover, the observed trend confirms what is expected from the gill–oxygen limitation theory [12], according to which fish body growth is limited by the gills' capability to provide oxygen through their surface. As oxygen solubility in water decreases with temperature [66], body size is expected to decrease, through phenotypic plasticity, to maintain the scope for aerobic activity. This hypothesis is further corroborated by the reduction in the condition factor, which is associated not only with low oxygen levels but also food limitations [67]. Furthermore, considering the potential effects of oxygen limitation on size at maturity, GSI, and egg production as well [68], it can thus be suggested that reproductive functions have undergone important changes over the last few decades. Unfortunately, no data about the reproductive traits were available from the 1990–1991 samples to test this phenomenon.

One interesting finding is that the timing of otolith seasonal depositions revealed a different pattern between the investigated periods. The edge-zone analysis pointed out a difference in the opaque deposition timing over the warm season, showing an opaque deposition rate > 90% from April to September in the 1990–1991 samples and from May to July in the 2020–2021 samples (no samples in August), therefore with a reduction in the length of the period. Several factors are known to influence the periodicity of opaque and translucent zones in otoliths, such as geographical distributions, life-history events (settlement and reproduction), food availability, and water temperature [69]. Nevertheless, temperature is known to play a primary role in determining deposition patterns [41,70,71], and consequently, the increased temperature may have affected the biomineralization process negatively.

Another possible explanation for the decreased growth performance may be related to another environmental driver, primary production, which has been recognized as one of the main historical drivers in the Mediterranean ecosystem [72]. For example, this is noticeable

in the AS, where forage fish population dynamics can be influenced by river discharge, and consequently, by primary production [73]. As a result, the declining trend in freshwater inputs observed in the Mediterranean Sea [74] could have played a significant role in the observed pattern, reducing the prey quantity or quality for mesopredatory species such as whiting.

We observed an unexpected outcome when comparing the LFDs by sex related to the marked sexual dimorphism in size featuring in the 2020–2021 sample. While in the 1990–1991 sample, the modal distributions of the two sexes mostly overlap (except for the largest length classes, dominated by females), a 5–6 cm gap was noticed between the sexes in TL modal classes in 2020–2021. As already reported for other areas, whiting females attain a larger size than males, showing higher L_∞ and lower k [75–77]. The increased difference in size may suggest a sex-dependent response related to the different energetic investments in gamete production and the effect of body size for each sex [78,79]. Although to our knowledge, a similar finding has never been pointed out in previous studies, we hypothesize that the integrated effect of fishing and warming towards smaller sizes exerts a stronger influence on males because of their lower reproductive cost with respect to females. On the other hand, females, despite being subjected to the same conditions, are less subjected to size decrease because their reproductive output (i.e., quantity and possibly quality of offspring) is positively correlated with size [79]. Another possible explanation could be related to modifications in energy uptake patterns between males and females, controlled by sex-specific behaviour, as already reported for whiting by [76]. Females ingest a significantly higher amount of food items and show lower percentages of empty stomachs compared to males. Fishing and warming could have acted in enhancing the degree of differentiation between these behavioral patterns, determining an increased dimorphism in growth rates over three decades.

Consideration must be made about the timing of the sample collection. Even if the same methodology was used, these results need to be interpreted with caution because of the longtime shift between sampling collection and its related issues. First, the samples came from two discrete sampling activities, thus providing detailed pictures of two restricted periods that were not appropriate to highlight a trend over three decades. The adaptive phenotypic plasticity may influence population dynamics even on a short-term scale, and it is favored by heterogeneous environments such as the AS [13]. Consequently, populations that are subjected to environmental variability may have natural oscillations in biological parameters in relation to external conditions. Finally, the skewed distribution observed in 1990–1991 is probably due to the higher proportion of specimens coming from the summer months, a period during which YOY are more abundant than adults [80]. In addition, it may be also related to the high fishing pressure exerted in the late 20th century, being the typical length structure featuring heavily exploited stocks [81].

4.2. Population Biological Traits

The size range found was smaller than that previously observed in the AS [31] and similar to the Black Sea [82,83]. As already reported for other gadoids [84], the Mediterranean maximum size was much smaller than the Atlantic one [76,85,86]. The presence of the opaque margin during the warmer months in the otoliths analyzed confirms the deposition pattern of the species, indicating that an opaque deposition is associated with the fast growth season [84,87,88].

The age classes and maximum age estimated in the present study were similar to those previously observed in the AS [30,80] and lower than those reported in the Atlantic Ocean and Black Sea [76,82,85,89]. Surprisingly, despite similar length ranges, our age estimates are lower than the Black Sea population, indicating faster growth and a shorter lifespan in the AS population. Moreover, this result is noticeable by comparing the growth rate and the growth performance between different areas, values of which in the AS population are the highest reported in the literature [46,77] (Figure 9). In particular, our estimates of *k* were higher than those previously reported probably because of the inclusion of the YOY data

in the VBGF, whose age estimation (in months) was validated through the analysis of the YOY LFDs collected between April and June (Figure A1). Generally, it is difficult to obtain length-at-age data of juvenile stages (when the growth rate reaches its maximum), and this often leads to an underestimation of k values [84]. Another explanation for the difference in the age–length results could be attributed to the different methodologies used to perform the age readings. After several attempts, we obtained consistent results with the "burnt and broken" otoliths, but there is no general agreement about the best method to use, even if the latest ICES guidelines [41] suggest using broken or sectioned preparations in this species. Additionally, age reading studies often lack a validation step (e.g., edge/length–frequency analysis, marking and recapturing, and tagging), limiting the comparability the results.
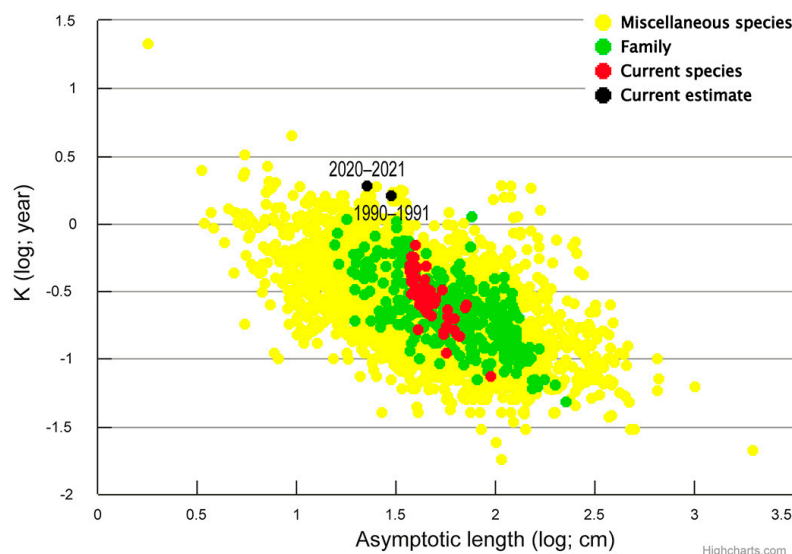
Figure 9. Auximetric plot for *Merlangius merlangus* and other gadid species that allows for comparison between the L_∞ and k estimated in this study (black) with other estimates obtained for the same species (red), other gadids (green), and other bony fish (yellow). Modified from [46].

Sexual maturity is reached within the first year of life in males and females at 16.1 and 16.8 cm TL, respectively. These estimates are lower than previous observations carried out in the AS [30,80] and, as expected, in the Atlantic Ocean [85]; on the other hand, our estimates were higher than those reported in the Black Sea [90]. The difference observed between our updated data and the previous studies in the AS agrees with our expectations, considering the reduction in L_∞ and the positive relationship between L_∞ and L_{50} [91]. Macroscopic observations on gonads and GSI trends indicated clearly that spawning takes place in winter, showing a narrower spawning season compared to the Atlantic Ocean and Black Sea, where it occurs from January to September and throughout the year, respectively [65,90]. During the spawning peak (December), the mean GSI value of the females (11%) is one order of magnitude higher than the males (1%), confirming the highly different reproductive efforts between the sexes [30,90].

The present study has provided fecundity estimates for the first time for whiting in the AS, which are within the range provided by previous studies carried out in the north east Atlantic Ocean and the Black Sea [65,92]. Considering that whiting is a batch spawner [52] and that the average F was 18.1 times higher than the average F_b, a female could potentially lay 18 batches during the spawning season. Regarding the OFDs, the presence of at least two separated modal groups was clear only in females in advanced ovarian developmental stages (with hydrated oocytes) and we often observed nonhomogeneous oocyte size distributions, without any recognizable modal group. Although whiting is considered to have a group-synchronous ovarian organization, our data suggest the possibility of an asynchronous organization [52], but the low number (15) of females used may not be adequate to infer the spawning pattern of this species.

The differences in life history traits observed between the Mediterranean Sea and Black Sea populations can be related to genetic divergence between them. Previous studies, based on morphological and meristic features, revealed differentiation between the AS and the Black Sea, raising a debate about the existence of two subspecies [93,94]. Recent molecular analyses have attempted to answer this question, stating that, despite some genetic differentiation between different sampling sites in the Black and Aegean Seas, there is no evidence supporting the existence of the presumed subspecies [95].

5. Conclusions

The present study provides a comprehensive picture of the biological life cycle and population parameters of the cold-water species *M. merlangus* in the AS. At the same time, it describes for the first time what seems to be a process of decreasing growth performance, depicting a current population composed of individuals with smaller sizes and lower body conditions than in 1990–1991. This process, together with the reduction in reproductive potential driven by the size dependency of fecundity values can lead to a more vulnerable and less resilient population, whose long-term stability is threatened by climate change and fishing exploitation. Surprisingly, we did not observe any difference in the age structure over the period considered, suggesting that fishing did not play a significant role in the observed species stock dynamics in the analyzed time period. On the other hand, our evidence indicates that modified environmental parameters (first of all sea temperature) may have led to the observed modification pattern, as already reported in several fish stocks worldwide [96]. Nevertheless, several questions about this phenomenon remain to be answered, for example, about the role of trophic ecology, which alone could explain such a growth variation through prey–predator interactions.

The study contributes to our understanding of the biological responses of fish populations to climate change and fishery impacts. Even if our data on whiting support that the main driver was represented by environmental pressures, it is well-known that interacting effects of climate change and fishing may be present, speeding up the declining trend of some groups of fish species, such as the cold-adapted ones living in the Mediterranean Sea [97,98]. Management policies need to consider these dynamics not only at the basin level but also at the local scale, providing adaptive measures based on the knowledge of interactions between the environment and the biota, which is the only way to achieve sustainable exploitation of fish resources.

Conflicts of Interest: The authors declare no conflict of interest.

Appendix A
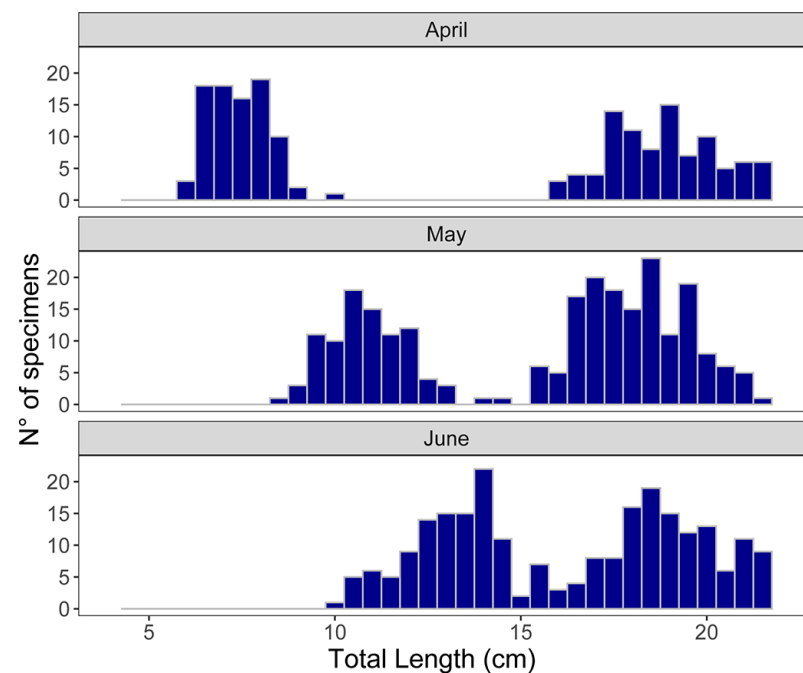
Figure A1. Monthly length–frequency distribution of *Merlangius merlangus* in the springtime of 2021. The bimodal distribution is due to the joining of the young-of-the-year (YOY) in the sampled population.
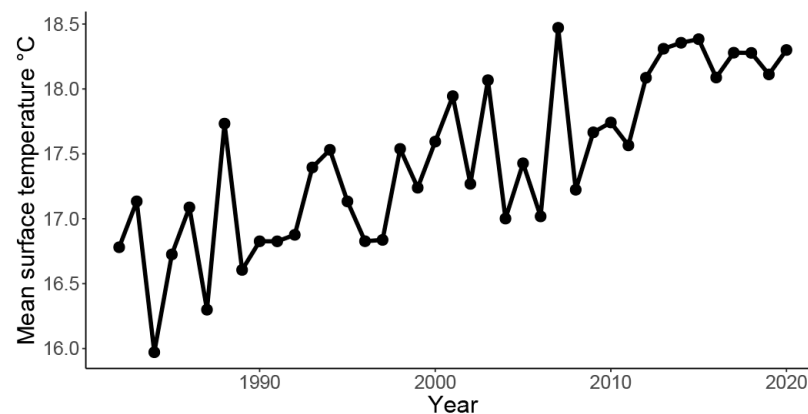
Figure A2. Historical trend of the mean annual values of surface temperature in the Adriatic Sea. Modified from [27].

Table A1. Age–length for females, males, and unsexed juveniles based on otolith readings of *Merlangius merlangus* sampled in the 1990–1991 period. N = total number; SD = standard deviation.

Age (Quarters)	Females											Males										
	6	9	12	15	18	21	24	27	30	33	N	6	9	12	15	18	21	24	27	30	33	N
Total length (cm)																						
12	1	1									2											0
13	6	2									8	5										5
14	12	6									18	8	7									15
15	2	4									6	4	4	2								10
16	3	4									7	2	4	2								8
17	3	4	2								9	4	4	2								10
18	3	4	2								9	4	4	3	2							13
19	4	4	2	1							11	4	4	4	2							14
20	3	4	2	2							11	2	4	6	2							14
21	2	4	4	2							12	2	4	5	4	1						16
22	2	3	4	2							11	1	4	3	3	1						12
23	1	3	4	2							10		4	4	4	2		1				15
24		3	3	2	1						9		1		3	3	1	3				11
25		1	2	2		1					6	1		2	1	2	2	2	1			11
26		3	7	3							13		1	1	2		2	3	1			10
27		1	3	5	2	1					12			1			2	2	1			7
28		1	2	2	1	1					7						2	1			1	4
29			1		2		1				4						1	1			1	3
30			1	1	2	1	1				6						1			1		2
31				1	2	1	1				5											0
32					2	2	3		1		8											0
33					1	1					2											0
34					1	1					2											0
35						1					1											0
37								1			1											0
N	42	52	39	25	14	10	6	1	1	-	190	37	45	35	23	15	8	11	3	1	2	180
TL mean (cm)	16.7	19.3	23.6	25.0	30.1	30.9	31.2	37.0	32.5	-		16.8	18.7	20.6	22.2	25.6	26.4	25.5	26.2	30.0	28.8	
TL SD	3.0	4.1	3.4	3.1	2.7	3.4	1.2	-	-	-		3.0	3.2	2.9	2.3	2.7	1.8	1.3	1.0	-	1.1	

Unsexed juveniles

Age (quarters)	3	6	9	12	N
Total length (cm)					
3	1				1
4	7				7
5	21				21
6	35				35
7	12				12
8	8				8
9	1	4			5
10	1	3			4
11		6			6
12		7			7
13		11	2		13
14		21	1		22
N	86	52	3	-	141
TL mean (cm)	6.3	12.8	13.5	-	
TL SD	1.2	1.6	0.5	-	

Table A2. Age–length for females, males, and unsexed juveniles based on otolith readings of *Merlangius merlangus* sampled in the 2020–2021 period. N = total number; SD = standard deviation.

Age (Quarters)	Females												Males											
	3	6	9	12	15	18	21	24	27	30	33	N	3	6	9	12	15	18	21	24	27	30	33	N
Total length (cm)																								
6	1											1	4											4
7	1											1	4	1										5
8	3	2										5	3											3
9	1	1										2	2											2
10		2										2	2											2
11		1										1		2										2
12												0		6										6
13		5										5		5			1							6
14		5	2	2	1							10		4		2	2							8
15		2	2	2	3							9		3	5	8	7	2						25

Table A2. *Cont.*

	Females												Males											
Age (Quarters)	3	6	9	12	15	18	21	24	27	30	33	N	3	6	9	12	15	18	21	24	27	30	33	N
16		4	2	4	4							14		3	4	6	8	2						23
17		4	4	5	4	1						18		4	4	7	7	2						24
18		2	4	6	7	2						21		2	3	5	8	4						22
19		1	3	5	5	2						16			2	7	5	5						19
20				4	6	4						20			4	3	4	6	1	3	1			22
21				3	6	5	1					22				2	3	4	1	3	2	1		16
22				4	5	7						23						3	2	2	2	1		10
23				1	4	6	4	1		1		17						1	1	4	1			7
24					3	3	4	1	1			12						1		1	1			3
25					2	3	6	1	3	2		17												0
26						1		2	3	1		8												0
27						2		5	2			9												0
28						1		1				2												0
29								1				1												0
30						1		1		1		3												0
31								1				1												0
32												0												0
33												0												0
34												0												0
35												0												0
36												0												0
37												0												0
N	6	29	29	50	57	40	3	15	9	2	-	240	15	30	22	40	46	29	5	13	7	2	-	209
TL mean (cm)	8.1	14.5	19.1	20.0	20.5	22.9	23.3	28.0	25.8	28.8	-		8.1	14.4	17.7	17.6	17.7	19.7	22.2	22.1	22.2	22.2	-	
TL SD	1.2	3.1	2.6	2.9	2.9	2.8	2.1	2.4	1.2	2.8	-		1.3	2.5	1.9	1.9	2.1	2.2	1.3	1.4	1.3	0.8	-	

Unsexed juveniles

Age (quarters)	3	6	9	12	N
Total length (cm)					
4	1				1
6	8				8
7	10				10
8	5				5
9	2	1			3
N	26	1	-	-	27
TL mean (cm)	7.4	9.3	-	-	
TL SD	1.1	-	-	-	

References

1. Micheli, F.; Halpern, B.S.; Walbridge, S.; Ciriaco, S.; Ferretti, F.; Fraschetti, S.; Lewison, R.; Nykjaer, L.; Rosenberg, A.A. Cumulative Human Impacts on Mediterranean and Black Sea Marine Ecosystems: Assessing Current Pressures and Opportunities. *PLoS ONE* **2013**, *8*, e79889. [CrossRef]
2. Cheung, W.W.L.; Watson, R.; Pauly, D. Signature of Ocean Warming in Global Fisheries Catch. *Nature* **2013**, *497*, 365–368. [CrossRef] [PubMed]
3. Azzurro, E.; Sbragaglia, V.; Cerri, J.; Bariche, M.; Bolognini, L.; Ben Souissi, J.; Busoni, G.; Coco, S.; Chryssanthi, A.; Fanelli, E.; et al. Climate Change, Biological Invasions, and the Shifting Distribution of Mediterranean Fishes: A Large-Scale Survey Based on Local Ecological Knowledge. *Glob. Chang. Biol.* **2019**, *25*, 2779–2792. [CrossRef]
4. Casini, M.; Bartolino, V.; Molinero, J.C.; Kornilovs, G. Linking Fisheries, Trophic Interactions and Climate: Threshold Dynamics Drive Herring *Clupea harengus* Growth in the Central Baltic Sea. *Mar. Ecol. Prog. Ser.* **2010**, *413*, 241–252. [CrossRef]
5. Pauly, D.; Christensen, V.; Dalsgaard, J.; Froese, R.; Torres, F. Fishing down Marine Food Webs. *Science* **1998**, *279*, 860–863. [CrossRef] [PubMed]
6. Barausse, A.; Michieli, A.; Riginella, E.; Palmeri, L.; Mazzoldi, C. Long-Term Changes in Community Composition and Life-History Traits in a Highly Exploited Basin (Northern Adriatic Sea): The Role of Environment and Anthropogenic Pressures. *J. Fish Biol.* **2011**, *79*, 1453–1486. [CrossRef]
7. Kuparinen, A.; Hutchings, J.A. Consequences of Fisheries-Induced Evolution for Population Productivity and Recovery Potential. *Proc. R. Soc. B Biol. Sci.* **2012**, *279*, 2571–2579. [CrossRef]
8. Fortibuoni, T.; Giovanardi, O.; Pranovi, F.; Raicevich, S.; Solidoro, C.; Libralato, S. Analysis of Long-Term Changes in a Mediterranean Marine Ecosystem Based on Fishery Landings. *Front. Mar. Sci.* **2017**, *4*, 33. [CrossRef]
9. Jackson, J.B.C.; Kirby, M.X.; Berger, W.H.; Bjorndal, K.A.; Botsford, L.W.; Bourque, B.J.; Bradbury, R.H.; Cooke, R.; Erlandson, J.; Estes, J.A.; et al. Historical Overfishing and the Recent Collapse of Coastal Ecosystems. *Science* **2001**, *293*, 629–637. [CrossRef]
10. Pauly, D.; Christensen, V.; Guénette, S.; Pitcher, T.J.; Sumaila, U.R.; Walters, C.J.; Watson, R.; Zeller, D. Towards Sustainability in World Fisheries. *Nature* **2002**, *418*, 689–695. [CrossRef]

11. Poloczanska, E.S.; Burrows, M.T.; Brown, C.J.; Molinos, J.G.; Halpern, B.S.; Hoegh-Guldberg, O.; Kappel, C.V.; Moore, P.J.; Richardson, A.J.; Schoeman, D.S.; et al. Responses of Marine Organisms to Climate Change across Oceans. *Front. Mar. Sci.* **2016**, *3*, 62. [CrossRef]

12. Pauly, D.; Cheung, W.W.L. Sound Physiological Knowledge and Principles in Modeling Shrinking of Fishes under Climate Change. *Glob. Chang. Biol.* **2018**, *24*, e15–e26. [CrossRef] [PubMed]

13. Hidalgo, M.; Olsen, E.M.; Ohlberger, J.; Saborido-Rey, F.; Murua, H.; Piñeiro, C.; Stenseth, N.C. Contrasting Evolutionary Demography Induced by Fishing: The Role of Adaptive Phenotypic Plasticity. *Ecol. Appl.* **2014**, *24*, 1101–1114. [CrossRef] [PubMed]

14. Free, C.M.; Thorson, J.T.; Pinsky, M.L.; Oken, K.L.; Wiedenmann, J.; Jensen, O.P. Impacts of Historical Warming on Marine Fisheries Production. *Science* **2019**, *365*, 979–983. [CrossRef] [PubMed]

15. Moullec, F.; Barrier, N.; Drira, S.; Guilhaumon, F.; Marsaleix, P.; Somot, S.; Ulses, C.; Velez, L.; Shin, Y.J. An End-to-End Model Reveals Losers and Winners in a Warming Mediterranean Sea. *Front. Mar. Sci.* **2019**, *6*, 345. [CrossRef]

16. Cheung, W.W.L.; Pauly, D. Impacts and Effects of Ocean Warming on Marine Fishes. In *Explaining Ocean Warming: Causes, Scale, Effects and Consequences*; Laffoley, D., Baxter, J.M., Eds.; IUCN: Gland, Switzerland, 2016; pp. 239–253.

17. Genner, M.J.; Sims, D.W.; Southward, A.J.; Budd, G.C.; Masterson, P.; Mchugh, M.; Rendle, P.; Southall, E.J.; Wearmouth, V.J.; Hawkins, S.J. Body Size-Dependent Responses of a Marine Fish Assemblage to Climate Change and Fishing over a Century-Long Scale. *Glob. Chang. Biol.* **2010**, *16*, 517–527. [CrossRef]

18. Hidalgo, M.; Rouyer, T.; Bartolino, V.; Cerviño, S.; Ciannelli, L.; Massutí, E.; Jadaud, A.; Saborido-Rey, F.; Durant, J.M.; Santurtún, M.; et al. Context-Dependent Interplays between Truncated Demographies and Climate Variation Shape the Population Growth Rate of a Harvested Species. *Ecography* **2012**, *35*, 637–649. [CrossRef]

19. Engelhard, G.H.; Righton, D.A.; Pinnegar, J.K. Climate Change and Fishing: A Century of Shifting Distribution in North Sea Cod. *Glob. Chang. Biol.* **2014**, *20*, 2473–2483. [CrossRef]

20. O'Connor, M.I.; Holding, J.M.; Kappel, C.V.; Duarte, C.M.; Brander, K.; Brown, C.J.; Bruno, J.F.; Buckley, L.; Burrows, M.T.; Halpern, B.S.; et al. Strengthening Confidence in Climate Change Impact Science. *Glob. Ecol. Biogeogr.* **2015**, *24*, 64–76. [CrossRef]

21. Coll, M.; Piroddi, C.; Albouy, C.; Ben Rais Lasram, F.; Cheung, W.W.L.; Christensen, V.; Karpouzi, V.S.; Guilhaumon, F.; Mouillot, D.; Paleczny, M.; et al. The Mediterranean Sea under Siege: Spatial Overlap between Marine Biodiversity, Cumulative Threats and Marine Reserves. *Glob. Ecol. Biogeogr.* **2012**, *21*, 465–480. [CrossRef]

22. Colloca, F.; Scarcella, G.; Libralato, S. Recent Trends and Impacts of Fisheries Exploitation on Mediterranean Stocks and Ecosystems. *Front. Mar. Sci.* **2017**, *4*, 244. [CrossRef]

23. Walther, G.R.; Post, E.; Convey, P.; Menzel, A.; Parmesan, C.; Beebee, T.J.C.; Fromentin, J.M.; Hoegh-Guldberg, O.; Bairlein, F. Ecological Response to Recent Climate Change. *Nature* **2002**, *416*, 389–395. [CrossRef] [PubMed]

24. Walther, G.R.; Roques, A.; Hulme, P.E.; Sykes, M.T.; Pyšek, P.; Kühn, I.; Zobel, M.; Bacher, S.; Botta-Dukát, Z.; Bugmann, H.; et al. Alien Species in a Warmer World: Risks and Opportunities. *Trends Ecol. Evol.* **2009**, *24*, 686–693. [CrossRef] [PubMed]

25. Bazairi, H.; Ben Haj, S.; Boero, F.; Cebrian, D.; De Juan, S.; Limam, A.; Lleonart, J.; Torchia, G.; Rais, C. *The Mediterranean Sea Biodiversity: State of the Ecosystems, Pressures, Impacts*; Unep-Map-Rac/Spa: Tunis, Tunisia, 2010; pp. 1–100.

26. Cardinale, M.; Scarcella, G. Mediterranean Sea: A Failure of the European Fisheries Management System. *Front. Mar. Sci.* **2017**, *4*, 72. [CrossRef]

27. García-Monteiro, S.; Sobrino, J.A.; Julien, Y.; Sòria, G.; Skokovic, D. Surface Temperature Trends in the Mediterranean Sea from MODIS Data during Years 2003–2019. *Reg. Stud. Mar. Sci.* **2022**, *49*, 102086. [CrossRef]

28. Tortonese, E. The Main Biogeographical Features and Problems of the Mediterranean Fish Fauna. *Copeia* **1964**, *1964*, 98–107. [CrossRef]

29. Ben Rais Lasram, F.; Guilhaumon, F.; Albouy, C.; Somot, S.; Thuiller, W.; Mouillot, D. The Mediterranean Sea as a "cul-de-Sac" for Endemic Fishes Facing Climate Change. *Glob. Chang. Biol.* **2010**, *16*, 3233–3245. [CrossRef]

30. Vallisneri, M.; Scapolatempo, M.; Tommasini, S. Reproductive Biology of *Merlangius merlangus*, L. (Osteichthyes, Gadidae) in the Northern Adriatic Sea. *Acta Adriat.* **2006**, *47*, 159–165.

31. Vallisneri, M.; Vecchi, A.; Manfredi, C. The Biological Cycle of *Merlangius merlangus* (Linnaeus, 1758) (Osteichthyes, Gadidae) in the Northern and Middle Adriatic Sea. *Biol. Mar. Medit.* **2004**, *11*, 652–656.

32. Reynolds, J.D.; Dulvy, N.K.; Goodwin, N.B.; Hutchings, J.A. Biology of Extinction Risk in Marine Fishes. *Proc. R. Soc. B Biol. Sci.* **2005**, *272*, 2337–2344. [CrossRef]

33. Russo, A.; Artegiani, A. Adriatic Sea Hydrography. *Sci. Mar.* **1996**, *60*, 33–43.

34. Hopkins, T.S. The Structure of Ionian and Levantine Seas. *Rep. Meteorol. Oceanogr.* **1992**, *41*, 35–36.

35. Ludwig, W.; Dumont, E.; Meybeck, M.; Heussner, S. River Discharges of Water and Nutrients to the Mediterranean and Black Sea: Major Drivers for Ecosystem Changes during Past and Future Decades? *Prog. Oceanogr.* **2009**, *80*, 199–217. [CrossRef]

36. Fonda Umani, S. Pelagic Production and Biomass in the Adriatic Sea. *Sci. Mar.* **1996**, *60*, 65–77.

37. Russo, A.; Carniel, S.; Sclavo, M.; Krzelj, M. Climatology of the Northern-Central Adriatic Sea. In *Modern Climatology*; Simon Wang, S.Y., Ed.; InTech: Rijeka, Croatia, 2012; pp. 177–212. [CrossRef]

38. Supić, N.; Grbec, B.; Vilibić, I.; Ivančić, I. Long-Term Changes in Hydrographic Conditions in Northern Adriatic and Its Relationship to Hydrological and Atmospheric Processes. *Ann. Geophys.* **2004**, *22*, 733–745. [CrossRef]

39. Kaschner, K.; Rius-Barile, J.; Kesner-Reyes, K.; Garilao, C.; Kullander, S.O.; Rees, T.; Froese, R. AquaMaps: Predicted Range Maps for Aquatic Species. Available online: www.aquamaps.org (accessed on 10 September 2022).

40. Bolger, T.; Connolly, P.L. The Selection of Suitable Indices for the Measurement and Analysis of Fish Condition. *J. Fish Biol.* **1989**, *34*, 171–182. [CrossRef]

41. Vitale, F.; Worsøe Clausen, L.; Nì Chonchuir, G. Handbook of Fish Age Estimation Protocols and Validation Methods. In *ICES Cooperative Research Report*; ICES: Copenhagen, Denmark, 2019; Volume 346. [CrossRef]

42. Campana, S.E. Accuracy, Precision and Quality Control in Age Determination, Including a Review of the Use and Abuse of Age Validation Methods. *J. Fish Biol.* **2001**, *59*, 197–242. [CrossRef]

43. Beamish, R.J.; Fournier, D.A. A Method for Comparing the Precision of a Set of Age Determinations. *Can. J. Fish. Aquat. Sci.* **1981**, *38*, 982–983. [CrossRef]

44. Chang, W.Y.B. A Statistical Method for Evaluating the Reproducibility of Age Determination. *Can. J. Fish. Aquat. Sci.* **1982**, *39*, 1208–1210. [CrossRef]

45. Kimura, D.K. Likelihood Methods for the von Bertalanffy Growth Curve. *Fish. Bull.* **1980**, *77*, 765–776.

46. Froese, R.; Pauly, D. FishBase. Available online: https://fishbase.mnhn.fr/popdyn/PopGrowthList.php?ID=29&GenusName=Merlangius&SpeciesName=merlangus&fc=183 (accessed on 10 December 2022).

47. *ICES CM 2007/ACFM:33*; Report of the Workshop on Sexual Maturity Staging of Cod, Whiting, Haddock and Saithe (WKM-SCWHS). ICES: Copenhagen, Denmark, 2008. [CrossRef]

48. Murua, H.; Kraus, G.; Saborido-Rey, F.; Witthames, P.R.; Thorsen, A.; Junquera, S. Procedures to Estimate Fecundity of Marine Fish Species in Relation to Their Reproductive Strategy. *J. Northwest Atl. Fish. Sci.* **2003**, *33*, 33–54. [CrossRef]

49. Choy, S.C. A Rapid Method for Removing and Counting Eggs from Fresh and Preserved Decapod Crustaceans. *Aquaculture* **1985**, *48*, 369–372. [CrossRef]

50. Pearson, A.G.E. *Histochemistry: Theoretical and Applied. Vol. 2: Analytical Technology*; Churchill Livingstone: Edinburgh, UK, 1985. [CrossRef]

51. Saber, S.; Macías, D.; Ortiz de Urbina, J.; Kjesbu, O.S. Stereological Comparison of Oocyte Recruitment and Batch Fecundity Estimates from Paraffin and Resin Sections Using Spawning Albacore (*Thunnus alalunga*) Ovaries as a Case Study. *J. Sea Res.* **2015**, *95*, 226–238. [CrossRef]

52. Murua, H.; Saborido-Rey, F. Female Reproductive Strategies of Marine Fish Species of the North Atlantic. *J. Northwest Atl. Fish. Sci.* **2003**, *33*, 23–31. [CrossRef]

53. Hunter, J.R.; Macewicz, B.J.; Chyan-Huei Lo, N.; Kimbrell, C.A. Fecundity, Spawning, and Maturity of Female Dover Sole Microstomus Pacificus, with an Evaluation of Assumptions and Precision. *Fish. Bull.* **1992**, *90*, 101–128.

54. Fisher, J.A.D.; Frank, K.T.; Leggett, W.C. Breaking Bergmann's Rule: Truncation of Northwest Atlantic Marine Fish Body Sizes. *Ecology* **2010**, *91*, 2499–2505. [CrossRef]

55. Bianchi, G.; Gislason, H.; Graham, K.; Hill, L.; Jin, X.; Koranteng, K.; Manickchand-Heileman, S.; Payá, I.; Sainsbury, K.; Sanchez, F.; et al. Impact of Fishing on Size Composition and Diversity of Demersal Fish Communities. *ICES J. Mar. Sci.* **2000**, *57*, 558–571. [CrossRef]

56. Shin, Y.J.; Rochet, M.J.; Jennings, S.; Field, J.G.; Gislason, H. Using Size-Based Indicators to Evaluate the Ecosystem Effects of Fishing. *ICES J. Mar. Sci.* **2005**, *62*, 384–396. [CrossRef]

57. Yemane, D.; Field, J.G.; Leslie, R.W. Indicators of Change in the Size Structure of Fish Communities: A Case Study from the South Coast of South Africa. *Fish. Res.* **2008**, *93*, 163–172. [CrossRef]

58. Edwards, C.T.T.; Plagányi, É.E. Protecting Old Fish through Spatial Management: Is There a Benefit for Sustainable Exploitation? *J. Appl. Ecol.* **2011**, *48*, 853–863. [CrossRef]

59. Pörtner, H.O.; Knust, R. Climate Change Affects Marine Fishes Through the Oxygen Limitation of Thermal Tolerance. *Science* **2007**, *315*, 95–97. [CrossRef]

60. Atkinson, D.; Sibly, R.M. Why Are Organisms Usually Bigger in Colder Environments? Making Sense of a Life History Puzzle. *Trends Ecol. Evol.* **1997**, *12*, 235–239. [CrossRef] [PubMed]

61. Pauly, D. Tropical Fishes: Patterns and Propensities. *J. Fish Biol.* **1998**, *53*, 1–17. [CrossRef]

62. Lindmark, M.; Ohlberger, J.; Gårdmark, A. Optimum Growth Temperature Declines with Body Size within Fish Species. *Glob. Chang. Biol.* **2022**, *28*, 2259–2271. [CrossRef]

63. Bianchi, C.N.; Morri, C. Marine Biodiversity of the Mediterranean Sea: Situation, Problems and Prospects for Future Research. *Mar. Pollut. Bull.* **2000**, *40*, 367–376. [CrossRef]

64. Bonacci, O.; Vrsalović, A. Differences in Air and Sea Surface Temperatures in the Northern and Southern Part of the Adriatic Sea. *Atmosphere* **2022**, *13*, 1158. [CrossRef]

65. Cohen, D.M.; Inada, T.; Iwamoto, T.; Scialabba, N. FAO Species Catalogue. Vol. 10. Gadiform Fishes of the World (Order Gadiformes). An Annotated and Illustrated Catalogue of Cods, Hakes, Grenadiers and Other Gadiform Fishes Known to Date. *FAO Fish. Syn.* **1990**, *125*, 319–327.

66. Forster, J.; Hirst, A.G.; Atkinson, D. Warming-Induced Reductions in Body Size Are Greater in Aquatic than Terrestrial Species. *Proc. Natl. Acad. Sci. USA* **2012**, *109*, 19310–19314. [CrossRef]

67. Casini, M.; Käll, F.; Hansson, M.; Plikshs, M.; Baranova, T.; Karlsson, O.; Lundström, K.; Neuenfeldt, S.; Gårdmark, A.; Hjelm, J. Hypoxic Areas, Density-Dependence and Food Limitation Drive the Body Condition of a Heavily Exploited Marine Fish Predator. *R. Soc. Open Sci.* **2016**, *3*, 160416. [CrossRef]

68. Kolding, J.; Haug, L.; Stefansson, S. Effect of Ambient Oxygen on Growth and Reproduction in Nile Tilapia (*Oreochromis niloticus*). *Can. J. Fish. Aquat. Sci.* **2008**, *65*, 1413–1424. [CrossRef]

69. Panfili, J.; de Pontual, H.; Troadec, H.; Wright, P.J. *Manual of Fish Sclerochronology*; Ifremer-lRD Coedition: Brest, France, 2002.

70. Choat, J.H.; Axe, L.M. Growth and Longevity in Acanthurid Fishes; An Analysis of Otolith Increments. *Mar. Ecol. Prog. Ser.* **1996**, *134*, 15–26. [CrossRef]

71. Fablet, R.; Pecquerie, L.; de Pontual, H.; Høie, H.; Millner, R.; Mosegaard, H.; Kooijman, S.A.L.M. Shedding Light on Fish Otolith Biomineralization Using a Bioenergetic Approach. *PLoS ONE* **2011**, *6*, e27055. [CrossRef]

72. Piroddi, C.; Coll, M.; Liquete, C.; Macias, D.; Greer, K.; Buszowski, J.; Steenbeek, J.; Danovaro, R.; Christensen, V. Historical Changes of the Mediterranean Sea Ecosystem: Modelling the Role and Impact of Primary Productivity and Fisheries Changes over Time. *Sci. Rep.* **2017**, *7*, 44491. [CrossRef]

73. Santojanni, A.; Arneri, E.; Bernardini, V.; Cingolani, N.; Di Marco, M.; Russo, A. Effects of Environmental Variables on Recruitment of Anchovy in the Adriatic Sea. *Clim. Res.* **2006**, *31*, 181–193. [CrossRef]

74. Macias, D.; Garcia-Gorriz, E.; Piroddi, C.; Stips, A. Biogeochemical Control of Marine Productivity in the Mediterranean Sea during the Last 50 Years. *Glob. Biogeochem. Cycles* **2014**, *28*, 897–907. [CrossRef]

75. Hussy, K.; Coad, J.O.; Farrell, E.D.; Clausen, L.W.; Clarke, M.W. Sexual Dimorphism in Size, Age, Maturation, and Growth Characteristics of Boarfish (*Capros aper*) in the Northeast Atlantic. *ICES J. Mar. Sci.* **2012**, *69*, 1729–1735. [CrossRef]

76. Lauerburg, R.A.M.; Keyl, F.; Kotterba, P.; Floeter, J.; Temming, A. Sex-Specific Food Intake in Whiting *Merlangius merlangus*. *J. Fish Biol.* **2015**, *86*, 1729–1753. [CrossRef]

77. Yildiz, T.; Saadet Karakulak, F. Age, Growth and Mortality of Whiting (*Merlangius merlangus*, Linnaeus, 1758) from the Western Black Sea, Turkey. *Turkish J. Fish. Aquat. Sci.* **2019**, *19*, 793–804. [CrossRef]

78. Hayward, A.; Gillooly, J.F. The Cost of Sex: Quantifying Energetic Investment in Gamete Production by Males and Females. *PLoS ONE* **2011**, *6*, e16557. [CrossRef] [PubMed]

79. Barneche, D.R.; White, C.R.; Marshall, D.J. Fish Reproductive-energy Output Increases Disproportionately With Body Size. *Science* **2018**, *645*, 642–645. [CrossRef] [PubMed]

80. Giovanardi, O.; Rizzoli, M. Biological Data, Collected during the Pipeta Expeditions, on the Whiting, *Merlangius merlangus* (L.) in the Adriatic Sea. *FAO Fish. Rep.* **1984**, *290*, 149–153.

81. Ottersen, G.; Hjermann, D.O.; Stenseth, N.C. Changes in Spawning Stock Structure Strengthen the Link between Climate and Recruitment in a Heavily Fished Cod (*Gadus morhua*) Stock. *Fish. Oceanogr.* **2006**, *15*, 230–243. [CrossRef]

82. Mazlum, R.E.; Bilgin, S. Age, Growth, Reproduction and Diet of the Whiting, *Merlangius merlangus euxinus* (Nordmann, 1840), in the Southeastern Black Sea. *Cah. Biol. Mar.* **2014**, *3*, 463–474.

83. Bilgin, S.; Bal, H.; Taşçı, B. Length Based Growth Estimates and Reproduction Biology of Whiting, *Merlangius merlangus euxinus* (Nordman, 1840) in the Southeast Black Sea. *Turkish J. Fish. Aquat. Sci.* **2012**, *12*, 871–881. [CrossRef]

84. Mir-Arguimbau, J.; Balcells, M.; Raventós, N.; Martín, P.; Sabatés, A. Growth, Reproduction and Their Interplay in Blue Whiting (*Micromesistius poutassou*, Risso, 1827) from the NW Mediterranean. *Fish. Res.* **2020**, *227*, 105540. [CrossRef]

85. Gerritsen, H.D.; Armstrong, M.J.; Allen, M.; McCurdy, W.J.; Peel, J.A.D. Variability in Maturity and Growth in a Heavily Exploited Stock: Whiting (*Merlangius merlangus*, L.) in the Irish Sea. *J. Sea Res. 49* **2003**, *49*, 69–82. [CrossRef]

86. Timmerman, C.A.; Marchal, P.; Denamiel, M.; Couvreur, C.; Cresson, P. Seasonal and Ontogenetic Variation of Whiting Diet in the Eastern English Channel and the Southern North Sea. *PLoS ONE* **2020**, *15*, e0239436. [CrossRef] [PubMed]

87. *ICES CM 1998/G:14*; Report of the Workshop on Otolith Ageing of North Sea Whiting. ICES: Copenhagen, Denmark, 1998. [CrossRef]

88. Ross, S.D.; Hüssy, K. A Reliable Method for Ageing of Whiting (*Merlangius merlangus*) for Use in Stock Assessment and Management. *J. Appl. Ichthyol.* **2013**, *29*, 825–832. [CrossRef]

89. Polat, N.; Gümücs, A. Ageing of Whiting (*Merlangius merlangus euxinus*, Nord., 1840) Based on Broken and Burnt Otolith. *Fish. Res.* **1996**, *28*, 231–236. [CrossRef]

90. Yildiz, T.; Uzer, U.; Yemişken, E.; Karakulak, F.S.; Kahraman, A.E.; Çanak, Ö. Conserve Immatures and Rebound the Potential: Stock Status and Reproduction of Whiting (*Merlangius merlangus* [Linnaeus, 1758]) in the Western Black Sea. *Mar. Biol. Res.* **2021**, *17*, 815–827. [CrossRef]

91. Pauly, D. Why Do Fish Reach First Maturity When They Do? *J. Fish Biol.* **2022**, *101*, 333–341. [CrossRef]

92. Ismen, A. Fecundity of Whiting, *Merlangius merlangus euxinus* (L.) on the Turkish Black Sea Coast. *Fish. Res.* **1995**, *22*, 309–318. [CrossRef]

93. Tortonese, E. *Fauna d'Italia*; Edizioni Calderini: Bologna, Italy, 1970.

94. Ungaro, N.; Marano, G.; Piccinetti, C. Adriatic, Black Sea: The Whiting Doubt. *Cybium* **1995**, *19*, 311–315.

95. Şalcıoğlu, A.; Gubili, C.; Krey, G.; Sönmez, A.Y.; Bilgin, R. Phylogeography and Population Dynamics of the Eastern Mediterranean Whiting (*Merlangius merlangus*) from the Black Sea, the Turkish Straits System, and the North Aegean Sea. *Fish. Res.* **2020**, *229*, 105614. [CrossRef]

96. Cheung, W.W.L.; Sarmiento, J.L.; Dunne, J.; Frölicher, T.L.; Lam, V.W.Y.; Palomares, M.L.D.; Watson, R.; Pauly, D. Shrinking of Fishes Exacerbates Impacts of Global Ocean Changes on Marine Ecosystems. *Nat. Clim. Chang.* **2013**, *3*, 254–258. [CrossRef]
97. Lloret, J.; Sabatés, A.; Muñoz, M.; Demestre, M.; Solé, I.; Font, T.; Casadevall, M.; Martín, P.; Gómez, S. How a Multidisciplinary Approach Involving Ethnoecology, Biology and Fisheries Can Help Explain the Spatio-Temporal Changes in Marine Fish Abundance Resulting from Climate Change. *Glob. Ecol. Biogeogr.* **2015**, *24*, 448–461. [CrossRef]
98. Lloret, J.; Serrat, A.; Thordarson, G.; Helle, K.; Jadaud, A.; Bruno, I.; Ordines, F.; Sartor, P.; Carbonara, P.; Rätz, H.J. The Poor Health of Deep-Water Species in the Context of Fishing Activity and a Warming Climate: Will Populations of Molva Species Rebuild or Collapse? *J. Fish Biol.* **2021**, *98*, 1572–1584. [CrossRef] [PubMed]